https://doi.org/10.2352/EI.2026.38.10.HVEI-227

Lightness-Based Spatially Adaptive Tone and Colorfulness Reproduction for HDR Imaging

Imran Mehmood[1], Brian Deegan[1] and Ming Ronnier Luo[2]
1. School of Engineering, University of Galway, Ireland.
2. State Key Laboratory of Extreme Photonics and Instrumentation, Zhejiang University, Hangzhou, China.

Abstract.

The existing tone mapping operators (TMOs), compress either the high dynamic range (HDR) image luminance or RGB channels and assume uniform adaptation conditions, contrary to human vision that adapts colorfulness under varying adaptation luminance conditions. One of the challenges in tone mapping is maintaining perceptual consistency of both lightness and colorfulness under varying adaptation luminance. Unlike traditional approaches, this work proposes CIECAM16 lightness based, spatially adaptive tone mapping and allows colorfulness according to local adaptation luminance. Furthermore, it uses spatial white point instead of a global one aligning the human perceptual phenomenon. The paper further analyzes the performance of the proposed TMO across various spatial conditions, demonstrating that it preserves local contrast and maintains detail in both highlight and shadow regions while adaptively regulating colorfulness under various adaptation conditions. Hence, this adaptive approach for HDR to standard dynamic range (SDR) mapping offers perceptually faithful representation.

Introduction

Real world exhibits a wider range of luminance and colors comprising HDR scenes which offer immersive visual experiences[1]. Capturing and displaying higher dynamic range contents present appealing imaging in photography, cinematic visualization and computer games. However, standard capturing and displaying devices have limitations in capturing full luminance range and color gamut as in the real world[2]. Latest HDR cameras are available, however the standard cameras capture full dynamic range with the help of bracketing features for the cameras. The tone mapping operators play significant role in compression of the dynamic range and enable the images to fit in with display dynamic range.

Several TMOs have been proposed over the years [3-10] however preserving the perceptual tone mapped image quality is a major challenge till date. Most of the TMOs compress the luminance of the HDR image such as Mantiuk's method [11], individual R, G, B channels such as Reinhard's[12]. These TMOs have been developed based on luminance histogram[13], bilateral filtering[14], or sigmoidal contrast compression methods while more recent approaches include convolutional neural network (CNNs) based models [9, 10]. While these models effectively compress the dynamic range, they often fail to perceptual color balance across varying adaptation conditions.

Color appearance models (CAM) such as CIECAM16[15], sCAM [16] and ZCAM [17] provide framework to predict color appearance attributes such as lightness (J), brightness (Q), colorfulness (M) and hue (h) under varying viewing and surround conditions. The CAMs predict various human visual system (HVS) effects such as Steven's and Hunt's effect. The input parameters to the CAMs include stimulus i.e., the physical color and surround conditions such as illuminance, background luminance, viewing environment and adaptation luminance and the output parameters include color appearance attributes including lightness, chroma and hue. CAM-based TMOs such as iCAM06 [7] and TMO_Z [8]. iCAM06 proposed by Fairchild et al. compresses individual independent coordinates i.e., X, Y, Z and incorporates various HVS phenomena. On the other hand, TMO_Z proposed by Luo et al. utilizes CIECAM16 perceptual coordinates compressing brightness and mapping optimal colors by incorporating surround and display conditions. TMO_Z improved the perceptual quality in terms of contrast, colorfulness and overall image quality leading to more optimal colors. iCAM06 assumes local adaptation while TMO_Z uses global adaptation to predict the perceptual attributes for each pixel.

The HVS has a color constancy mechanism that is strongly influenced by adaptation luminance and contributes to maintaining stable color appearance under varying adaptation luminance. In CIECAM16, brightness can vary non-intuitively under spatially varying adaptation luminance, which may reduce perceptual consistency in tone-mapping applications. When brightness is constant and adaptation luminance (L_a) is decreased, the adaptation factor (F_L) decreases. Since lower F_L increases response compression, chroma and colorfulness decrease which directly follows from CIECAM16 formulation. In contrast, when the lightness is kept constant with increasing L_a, the F_L increases, reducing response compression and increasing effective chroma which in turn increases perceived colorfulness, making colors appear more vivid. Figure 1 illustrates the relationship between L_a, F_L, colorfulness and lightness gains. As the L_a increases, the F_L increases. The colorfulness gain increases for constant lightness while it decreases for constant brightness, consistent with psychophysical studies reported as in [18].

The phenomenon described above emphasizes the significance of utilizing perceptual lightness for tone mapping. This paper proposes the lightness based perceptual tone mapping operator (LTMO) that utilizes the CIECAM16 based perceptual lightness rather than brightness and predicts colorfulness in

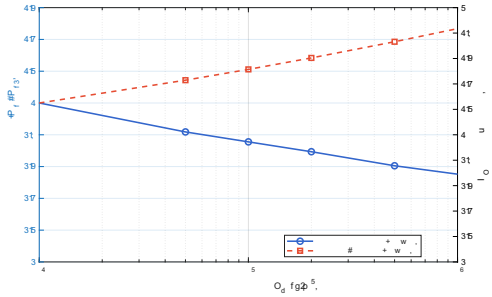

***Figure 1**. The colorfulness gain and adaptation factor vs adaptation luminance.*

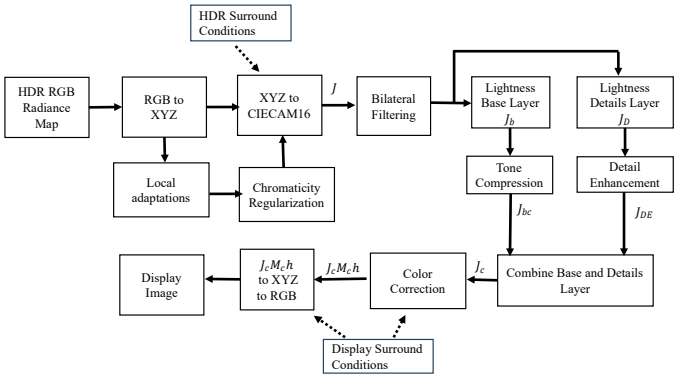

***Figure 2**. The workflow of proposed model.*

consistent with perceptual behavior under varying adaptation conditions. Moreover, the LTMO uses a local white point, adaptation luminance, and background luminance. Since spatial white point for the displays is not convenient, global display white point is used that may result in color cast over entire images. This paper also investigates the effects of global versus local white points and proposes a method for regulating the local white point to minimize color-cast artifacts.

Methodology

The workflow for the LTMO follows the general framework of TMO_Z [8], but modifies perceptual attributes to maintain consistency with human visual system (HVS) adaptation mechanisms. The flowchart is shown in Fig. 2. The input to the model is an HDR RGB radiance map, which is converted into HDR XYZ data. Since the RGB radiance map is typically linear, the RGB to XYZ transformation can be applied using a camera characterization model without non-linearity mapping.

The XYZ-to-CIECAM16 transformation requires viewing conditions: the white point W, adaptation luminance L_a, background luminance Y_b, and surround type (dim, dark, or average). Two types of viewing conditions are used here: one for computing CIECAM16 color appearance attributes of the HDR image, and the other for calculating colorfulness under varying display adaptation luminance.

We denote the global white point as $W_g = [X_w, Y_w, Z_w]$and the local white point as $W_l = [X_{wl}, Y_{wl}, Z_{wl}]$.

Spatial adaptations

The HDR XYZ to CIECAM16 processing uses a spatially varying local white point $W_\ell(x,y)$, calculated following Fairchild[7]:

$$W_{H\ell}(x,y) = (I * G_\sigma)(x,y) \tag{1}$$

where $W_{H\ell}(x,y)$is the local white point for the HDR-to-CIECAM16 transformation, $I(x,y) = [X_H, Y_H, Z_H]$ are the XYZ channels of the input image, G_σ is a 2D Gaussian kernel controlling the adaptation neighborhood, and $*$ denotes convolution applied independently to each channel. The standard deviation σ determines the extent of local adaptation and it was set to 2% of the image size.

Since the display white point $W_{d,g}$ is typically global, processing purely with local white points and then transforming back to RGB using a global white can introduce color casts. To prevent this, local white points are regularized using chromaticity regularization.

Let $c_{H\ell} = W_{H\ell}/Y_{H\ell}$ and $c_g = W_g/Y_g$. The local chromaticity is blended with the global chromaticity using a luminance-driven factor $\beta(x,y)$:

$$\beta(x,y) = \frac{Y_{H\ell}(x,y)}{Y_{H\ell}(x,y)+k}, k = \alpha\, Y_g \tag{3}$$

The new chromaticity can be calculated using equation (4).

$$c'(x,y) = c_g + \beta(x,y)\,(c_\ell(x,y) - c_g) \tag{4}$$

The c_g equals to W_g/Y_g. The blending parameter $\beta(x,y)$ acts as a luminance-dependent control that determines how much of the local color information should be retained. In dark regions, noise and illumination variations make local chroma unstable, while in bright regions, the local chromaticity is more accurate. Therefore, $\beta(x,y)$ acts as a smoothing function of the local chromaticities, so that the transition between global and local color influence occurs gradually. The final local white point can be reconstructed as:

$$W'_{H\ell}(x,y) = Y_\ell(x,y) \cdot c'(x,y) \tag{5}$$

The $W'_{H\ell}(x,y)$ enables to keep $Y_{H\ell}$, L_a and Y_b fully spatial to handle spatially varying adaptation while ensuring color constancy without changing the fundamental local adaptation estimates. The β based regularization pulls dark regions toward the global white point preventing strong tints in shadows. The global white point (W_g) acts as a stable anchor and avoids the local white drift that happens if local estimates are wrong. The effects β will be discussed in results section.

Following Fairchild and Luo, the HDR adaptation luminance $L_{a,H\ell}$ is set to 20% of the local luminance Y_{Hl}, and the background luminance $Y_{b,H\ell}$ is set to 20% of $L_{a,H\ell}$ [19, 20].

Lightness Computation

To calculate lightness of the HDR image, the achromatic responses of the stimulus and white point are computed. Since the image is HDR therefore previously computed white point, $W'_{H\ell}(x,y)$ i.e., $[X_{w,H\ell}, Y_{w,H\ell}, Z_{w,H\ell}]$, and spatial L_{aH} and Y_{bH} will be used for the forward transformations.

$$\begin{pmatrix} R_{w,H} \\ G_{w,H} \\ B_{w,H} \end{pmatrix} = M_{CAT16} \begin{pmatrix} X_{w,H\ell} \\ Y_{w,H\ell} \\ Z_{w,H\ell} \end{pmatrix} \tag{6}$$

Calculate the degree of adaptation, D_T.

$$D_H = F\left[1 - \left(\frac{1}{3.6}\right) exp\left(\frac{-L_{aH}-42}{92}\right)\right] \tag{7}$$

Other parameters are computed following standard CIECAM16 equations, including:

$$D_{R,H}(x,y) = D\frac{Y_{w,H\ell}}{R_{w,H\ell}} + 1 - D_{H\ell} \tag{8}$$

$$F_{L,H} = 0.2k^4(5L_{a,H\ell}) + 0.1(1-k_H^4)^2(5L_{a,H\ell})^{1/3}$$

where $k_H = \frac{1}{5L_{a,H\ell}+1}$ and

$$\begin{pmatrix} R_{WC,H} \\ G_{WC,H} \\ B_{WC,H} \end{pmatrix} = \begin{pmatrix} D_{R,H}R_{w,H} \\ D_{G,H}G_{w,H} \\ D_{B,H}B_{w,H} \end{pmatrix} \quad (9)$$

$$R_{aW,H} = 400\left(\frac{(x)^{0.42}}{(x)^{0.42}+27.13}\right) + 0.1 \quad (10)$$

where $x = F_{L,H}\, R_{WC,H}/100$. Similarly, calculate the $G_{aW,H}$ and $B_{aW,H}$ by replacing $R_{WC,H}$ with $G_{WC,H}$ and $B_{W,CH}$, respectively. Now, calculate the achromatic response for the white point:

$$A_{W,H} = \left[2R_{aW,H} + G_{aW,H} + 0.05B_{aW,H} - 0.305\right]N_{bb} \quad (11)$$

Apply the formulation (6)-(10) on the HDR image XYZ to get A_H as in (12).

$$A_H = [2R_{aH} + G_{aH} + 0.05B_{aH} - 0.305]N_{bb} \quad (12)$$

Finally, the lightness of the tone-mapped image is computed using (8).

$$J_H = 100\left(\frac{A_{H\ell}}{A_{wH\ell}}\right)^{c.z} \quad (13)$$

where parameters c, z, N_c, N_{cb} follow the standard CIECAM16 equations.

Tone Mapping

In this study, lightness channel is used for tone mapping. The HDR lightness $\boldsymbol{J_H}$ is normalized with maximum lightness ($\boldsymbol{J_{Hmax}}$) and decomposed into low pass and high pass images resulting in base and details layers. The base layer is compressed, and detail layer is enhanced. In literature, multiple filters are available to separate low pass and high pass contents including Gaussian's and Bilateral filters [14]. The generic gaussian filter introduces halos in the resultant images therefore Bilateral filter was used to separate the base $\boldsymbol{J_b}$ and details layers $\boldsymbol{J_E}$ as follows:

$$J_b = \frac{1}{k(s)}\sum_{p\in\Omega} f(p-s)g\left(J_{Hp} - J_{Hs}\right)J_{Hp} \quad (14)$$

Where $k(s)$ normalizes each pixel is defined as

$$k(s) = \sum_{p\in\Omega} f(p-s)g\left(J_{Hs} - J_{Hp}\right) \quad (15)$$

where $f(\cdot)$ and $g(\cdot)$ are spatial domain Gaussian filters and brightness domain filters with standard deviations σ_s and σ_r, respectively. The J_{Hs} is the lightness at each pixel s. The bilateral filter controls the sharpness of the edges using standard deviations. The σ_s is set to 2% of the image size while the value of the σ_r is set to a constant value of 0.35.

The output of the bilateral filter is the base layer J_b and the details layer J_D of the lightness channel was calculated by subtracting the lightness base layer from original lightness J_H in log domain. The two layers are combined back after the following processing.

To test the performance of lightness based tone mapping, simple global tone compression method was used that is defined by

$$J_{bc} = J_b^{\gamma}, \qquad \gamma \in [0\ 1] \quad (15)$$

As the value of γ decreases the compression in contrast increases and vice versa. The authors experimented with various values of gamma to set gamma adaptive and found empirically that $\gamma = ak + b$ where k is the key of the image [5], a= 0.6581 and b= 0.4128. The key of the image is the gematric mean of the original HDR lightness i.e., J_H.

Since the base layer of the lightness is compressed, the edges of the original images get distorted. Hence the details layers need to be enhanced. The details layer was enhanced as follows:

$$J_{DE} = D_{\mathrm{D,max}}\left(\frac{|J_D|}{J_{\mathrm{D,max}}}\right)^{\delta} \times \mathrm{sgn}[J_D] \quad (16)$$

Where J_{DE} is the enhanced detail layer and δ is the detail enhancement parameters. The value of the δ for most of the images was set at 1.1. The tone mapped lightness base layer and details enhanced detail layer is combined using $J_c = J_{\mathrm{Hmax}}(J_{bc}\, J_{DE})$ to get final tone mapped lightness.

Color Correction

Following the recipe of [8], the hue of the tone mapped image was directly calculated from the HDR image. However, to compute new colorfulness under display surround conditions, display surround parameters are required. Since the displays are typically designed homogeneous with white point and a global display whit point is used therefore to compute the colorfulness for the display, a global display white point $W_{dg} = \left[x_{w,dg}, y_{w,dg}, z_{w,dg}\right]$ was used. The adaptation luminance $L_{a,dg}$ and background luminance $Y_{b,dg}$ were used. It is to note that $L_{a,dg}$ can be set to see effect of colorfulness under varying $L_{a,dg}$. As described earlier, varying $L_{a,dg}$ should also impact on the colorfulness. The hue of the image can be as follows.

$$a_H = R_{aH} - \frac{12\cdot G_{aH}}{11} + \frac{B_{aH}}{11}$$
$$b_H = \frac{R_{aH}+G_{aH}+2B_{aH}}{9} \quad (17)$$

$$h_H = tan^{-1}(b_H/a_H) \quad (18)$$

where a_H and b_H are intermediate opponent color components defining red–green and yellow–blue direction and h_H is the final hue of the image.

To calculate colorfulness, compressed lightness J_c can be directly used in the equations in the following equation.

$$C_c = t^{0.9}\left(\frac{J_c}{100}\right)^{0.5}(1.64 - 0.29^n)^{0.73} \quad (19)$$

$$M_c = C_c F_{L,dg} \quad (20)$$

and

$$e_t = \frac{1}{4}\cdot\left[cos\left(\frac{h_H\cdot\pi}{180}+2\right)+3.8\right] \quad (21)$$

$$t = \frac{\left(\frac{50000}{13}\cdot N_c\cdot N_{cb}\right)\cdot e_t\cdot\left(a_H^2+b_H^2\right)^{1/2}}{R_{aH}+G_{aH}+\left(\frac{21}{20}\right)\cdot B_{aH}} \quad (22)$$

$F_{L,dg}$ is computed using display adaptation conditions i.e., $L_{a,dg}$ and $Y_{b,dg}$.

Display Image Transformation

In CIECAM16, the viewing conditions are defined by four parameters: the surround type (average, dim, or dark), illuminant, adaptation luminance L_a, and background luminance Y_b. Since cameras do not directly measure L_a and Y_b, these values are typically estimated from the average scene luminance and viewing conditions. Following the recommendations in CIE Technical Report 159:2004 and the studies by Fairchild and Luo [20], Y_b is set to 20 for average surround, while L_a is approximated as 20–80 cd/m² depending on the illumination level. In this work, we used $L_{AH} = 0.2\, L_{H,max}$, $Y_{b,dg} = 20$, D65 display white point and $L_{A,dg}$ was varied to see colorfulness effects.

Lastly, the inverse CIECAM16 model is used to convert the tone compressed lightness, colorfulness, and hue (J_C, M_c, h_H) into XYZ coordinates. The display surround conditions are used in the inverse transformation. The luminance values of 1% of the pixels are clipped to create the simulation of glare. The XYZ to sRGB transformation or a specific display characterization model, like the GOG [21] model, are then used to convert the resultant XYZ image into RGB images. The sRGB color space is used to display images in this paper.

Results and Discussion

The performance of the proposed algorithm was analyzed to evaluate the impact of lightness-based tone mapping under varying adaptation conditions. The evaluation in this work is primarily qualitative, focusing on visual consistency and perceptual plausibility under varying adaptation luminance. While objective metrics such as TMQI [22] can provide useful supporting signals for naturalistic contrast, they imperfectly correlate with perceptual attributes such as colorfulness and adaptation-dependent appearance. For this reason, we emphasize visual analysis grounded in established HVS behavior. Figures 3 and 4 illustrate the results for different values of the adapting luminance L_a. As the adaptation level increases, the perceived brightness and colorfulness of the scene also increase, demonstrating the strong dependence of chromatic adaptation on L_a. For low adaptation levels (e.g., $L_a = 10$), the image appears darker and less saturated, consistent with the limited visual sensitivity of the HVS under low-light (mesopic) conditions. The image in Figure 3 is darker compared to Figure 4, reflecting the need for a lower adaptation luminance and correspondingly lower colorfulness. Conversely, the scenes in Figure 4 require higher colorfulness as the scene is very bright. As L_a increases to 100 or beyond, the colors become gradually more vivid, and the overall contrast improves, closely reflecting photopic visual response.

This behavior aligns with characteristics of the human visual system (HVS), where higher adaptation luminance levels correspond to greater sensitivity to chromatic differences and increased perceived colorfulness. The gradual enhancement of saturation and brightness observed confirms that the proposed tone-mapping algorithm accurately models adaptation-dependent color response. Furthermore, the absence of visible color artifacts or tonal discontinuities indicates that the algorithm maintains stable color balance and smooth transitions across luminance levels. Overall, these results validate the effectiveness of the proposed method in reproducing perceptually realistic colors across a wide range of adaptation luminances.

Further, the performance was investigated under four different scenarios to evaluate the impact of global and local adaptation parameters on chromatic appearance and tone mapping. In the first case, the β was set to zero, the local chromaticity was completely discarded, and the pixel adopted the chromaticity of the global white point, which means all adaptation parameters, including the white point, the adaptation luminance (L_a), and the background luminance (Y_b), were set globally. The tone mapped image is presented in Figure 5(a). This case corresponds to the uniform global adaptation model, where every pixel in the image is referenced to the same global white point. The primary advantage of this approach is its robustness against color casts, as it enforces a consistent global reference across the scene.

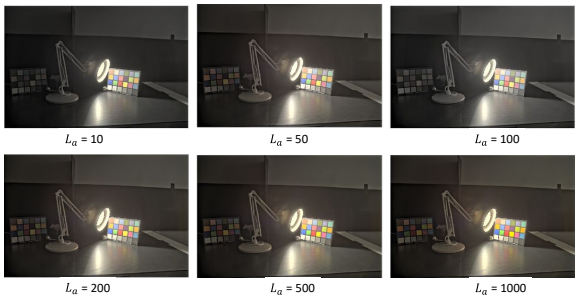

Figure 3. *Performance of proposed TMO under different display adaptation luminance ($L_{a,dg}$) conditions.*

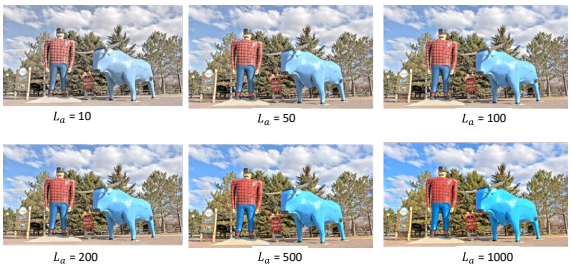

Figure 4: *Performance of proposed TMO under different adaptation luminance ($L_{a,dg}$) conditions.*

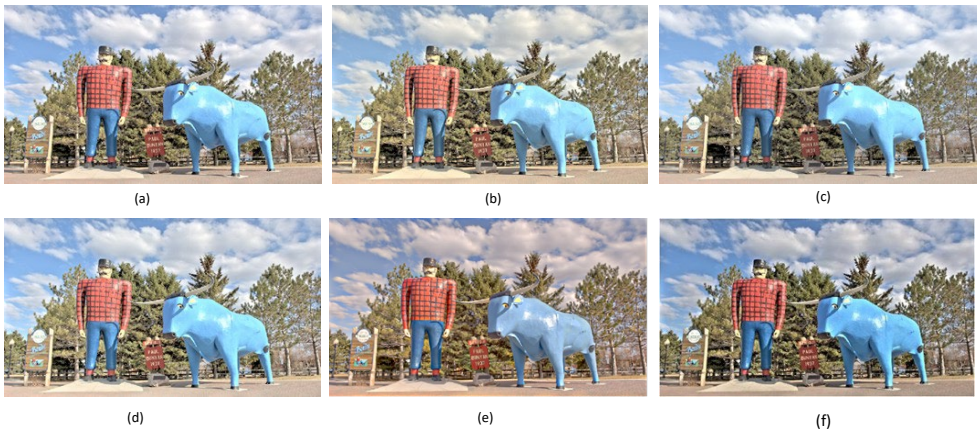

Figure 5: *Comparison of the proposed method under different cases. (a): Global conditions. (b): Spatial conditions (c) white point global but La and Yb are local (d) chromaticity regularized white point and spatial L_a and Y_b (e) iCAM06 (f) TMOz.*

However, because spatial variations in illumination are ignored, this method does not represent spatial white-point effects as modeled in CAMs.

In the second case, the β was set to 1, retaining full local chromaticity without influence from the global white including $w_H(x,y)$, $L_{a,H}$ and $Y_{b,H}$. This approach is better suited for scenes containing mixed or spatially varying illumination, as it allows each region to adapt according to its own local lighting conditions. Consequently, the rendered colors appear more faithful to the actual scene, particularly in regions affected by color casts or varying light sources. However, since the display white point is set globally, color casts occurred due to a mismatch between spatial and global transformations, as depicted in Figure 5(b). The same color cast can be seen in iCAM06 (Figure 5(e)), since iCAM06 deals with local adaptation throughout processing while using global white point for transforming to the display image. However, TMO_z in Figure 5(f) uses global white points in both forward and inverse transformations; therefore, there is no color cast.

The third scenario represents a mixed approach in which the global white point is maintained while the local adaptation parameters ($L_{a,H\ell}$ and $Y_{b,H\ell}$) are allowed to vary spatially as depicted in Figure 5(c). This mechanism aims to preserve the perceptual consistency of local adaptation luminance while anchoring all colors to a common global chromatic reference. The main advantage of this setup is that it eliminates color casts that arise from local to global while still accounting for variations in viewing and background luminance. However, the limitation is that it does not employ a spatially varying white point, as considered in the full CIECAM16 formulation, and thus underrepresents true localized color adaptation under strongly varying lighting.

In the last case, the chromaticity regularized white point approach defined in equations (4) and (5) was used with $\alpha = 0.6$, in which the local luminance and adaptation parameters (Y_{Hl}, $L_{a,H\ell}$, $Y_{b\ell}$) are preserved, but chromaticities are partially mapped toward the global white chromaticity to minimize the color cast effect, as seen in Figure 5(d). It can be noticed that this version appears more natural, since the other two images in Figures (a) and (c) tend toward the D65 white point.

Figure 6 depicts the mapping of local chromaticity toward global chromaticities in CIE 1976 u′v′ diagram. The subfigure is the zoomed version. The red colors correspond to the original chromaticity values, the blue represents the mapped values, the yellow star indicates the global white-point chromaticity, while the black vectors pointing from the red points to the blue points represent the mapping vectors. Figure 7 shows the magnitudes of the chromaticity shifts in Figure 6. Since, in dark regions, the colors appear less chromatic, the required shift is lower compared to bright regions. Hence, the algorithm shifts darker chromaticities with lower magnitudes, preserving local chromaticity in the overall image. In dark regions, the algorithm naturally favors the global white (reducing noise and unwanted tints), while in bright regions, it shifts more toward global chromaticities. Therefore, the proposed algorithm effectively combines the strengths of both global and local adaptation, resulting in perceptually reasonable and color-balanced images across varying illumination conditions.

Figure 8 presents comparisons of the proposed method with other TMOs. The TMO-NET [10], DeepTMO[9], Hui[3], Liang [4], and Reinhard TMO [6] do not use any adaptation mechanism. The TMO_z uses the D65 white point for processing, while iCAM06 and the proposed method use spatial white points and adaptation conditions. It is evident that the proposed model retains

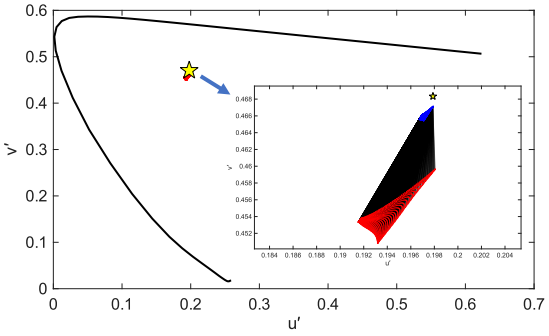

Figure 6: *Chromaticity shifts toward global white point. The subfigure is the zoomed version.*

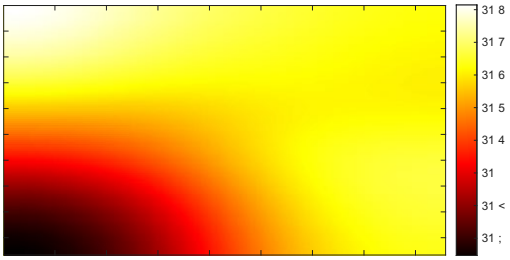

Figure 7: *magnitudes of chromaticity shifts.*

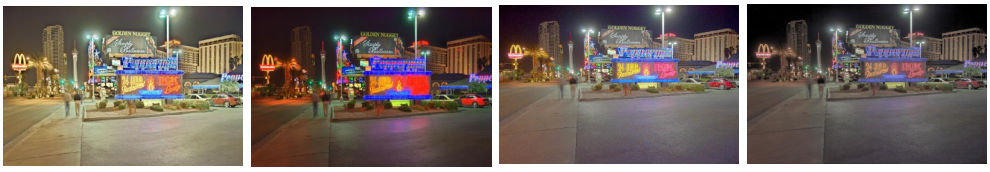

(a) TMO-NET (i) DeepTMO (c) Hui (d) Liang

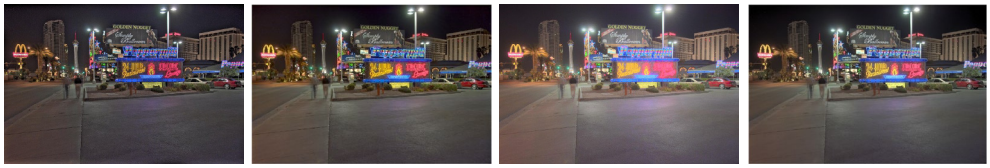

(j) TMOz (j) iCAM06 (f) Reinhard (G) LTMO (Proposed)

Figure 8: *Comparison of the proposed model with other TMOs.*

color balance and presents natural contrast, resulting in a natural and visually pleasing appearance of the image.

Conclusions

This paper presents a lightness-based, spatially adaptive tone and colorfulness reproduction model for HDR imaging that leverages the perceptual attributes of the CIECAM16 color appearance model. Unlike conventional tone mapping operators that assume uniform adaptation and compress only luminance or RGB channels, the proposed LTMO maintains perceptual consistency by adapting colorfulness according to local adaptation luminance while using lightness as the tone mapping parameter. The integration of spatially adaptive white points and chromaticity regularization effectively minimizes color casts and preserves local contrast, highlight, and shadow details across varying adaptation conditions. Overall, the LTMO offers a perceptually faithful and adaptive solution for HDR to SDR mapping, aligning more closely with the HVS response to lightness and colorfulness under varying luminance conditions. In the future, Naka-Rushton–based tone curves will be studied, and the contrast will also be adapted according to the adaptation conditions. A comprehensive subjective study and quantitative benchmarking will be considered in future work to compare LTMO with other TMOs under various lighting conditions.

Acknowledgement

This publication has emanated from research jointly funded by Taighde Éireann – Research Ireland under Grant Number 13/RC/2094_2, and co-funded by the European Union under the Systems, Methods, Context (SyMeCo) programme Grant Agreement Number 101081459. Views and opinions expressed are however those of the author(s) only and do not necessarily reflect those of the European Union or the European Research Executive Agency. Neither the European Union nor the granting authority can be held responsible for them.

References

[1] A. K. Venkataramanan and A. C. Bovik, "Subjective quality assessment of compressed tone-mapped high dynamic range videos," *IEEE Transactions on Image Processing,* 2024.

[2] Q. Jiang, X. Li, X. Wang, Z. Wang, and G. Zhai, "Dataset and Metric for Quality Assessment of HDR Tone Mapping: Detail Visibility, Color Naturalness, and Overall Quality," *IEEE Transactions on Multimedia,* 2025.

[3] H. Li, X. Jia, and L. Zhang, "Clustering based content and color adaptive tone mapping," *Computer Vision and Image Understanding,* vol. 168, pp. 37-49, 2018.

[4] Z. Liang, J. Xu, D. Zhang, Z. Cao, and L. Zhang, "A hybrid l1-l0 layer decomposition model for tone mapping," in *Proceedings of the IEEE conference on computer vision and pattern recognition*, pp. 4758-4766, 2018.

[5] E. Reinhard, "Parameter estimation for photographic tone reproduction," *Journal of graphics tools,* vol. 7, no. 1, pp. 45-51, 2002.

[6] E. Reinhard, M. Stark, P. Shirley, and J. Ferwerda, "Photographic tone reproduction for digital images," in *Proceedings of the 29th annual conference on Computer graphics and interactive techniques*, pp. 267-276, 2002.

[7] J. Kuang, G. M. Johnson, and M. D. Fairchild, "iCAM06: A refined image appearance model for HDR image rendering," *Journal of Visual Communication and Image Representation,* vol. 18, no. 5, pp. 406-414, 2007.

[8] I. Mehmood, X. Shi, M. U. Khan, and M. R. Luo, "Perceptual tone mapping model for high dynamic range imaging," *IEEE Access,* vol. 11, pp. 110272-110288, 2023.

[9] A. Rana, P. Singh, G. Valenzise, F. Dufaux, N. Komodakis, and A. Smolic, "Deep tone mapping operator for high dynamic range images," *IEEE Transactions on Image Processing,* vol. 29, pp. 1285-1298, 2019.

[10] K. Panetta, L. Kezebou, V. Oludare, S. Agaian, and Z. Xia, "Tmo-net: A parameter-free tone mapping operator using generative adversarial network, and performance benchmarking on large scale hdr dataset," *IEEE Access,* vol. 9, pp. 39500-39517, 2021.

[11] R. Mantiuk, S. Daly, and L. Kerofsky, "Display adaptive tone mapping," in *ACM SIGGRAPH 2008 papers*, 2008, pp. 1-10.

[12] E. Reinhard and K. Devlin, "Dynamic range reduction inspired by photoreceptor physiology," *IEEE transactions on visualization and computer graphics,* vol. 11, no. 1, pp. 13-24, 2005.

[13] I. R. Khan, S. Rahardja, M. M. Khan, M. M. Movania, and F. Abed, "A tone-mapping technique based on histogram using a sensitivity model of the human visual system," *IEEE Transactions on Industrial Electronics,* vol. 65, no. 4, pp. 3469-3479, 2017.

[14] F. Durand and J. Dorsey, "Fast bilateral filtering for the display of high-dynamic-range images," in *Proceedings of the 29th annual conference on Computer graphics and interactive techniques*, pp. 257-266, 2002.

[15] C. Li *et al.*, "Comprehensive color solutions: CAM16, CAT16, and CAM16-UCS," *Color Research & Application,* vol. 42, no. 6, pp. 703-718, 2017.

[16] M. Li and M. Luo, "Simple color appearance model (sCAM) based on simple uniform color space (sUCS)," *Optics Express,* vol. 32, no. 3, pp. 3100-3122, 2024.

[17] M. Safdar, J. Y. Hardeberg, and M. Ronnier Luo, "ZCAM, a colour appearance model based on a high dynamic range uniform colour space," *Optics Express,* vol. 29, no. 4, pp. 6036-6052, 2021.

[18] L. Hellwig and M. D. Fairchild, "Brightness, lightness, colorfulness, and chroma in CIECAM02 and CAM16," *Color Research & Application,* vol. 47, no. 5, pp. 1083-1095, 2022.

[19] M. R. Luo and C. Li, "CIECAM02 and its recent developments," in *Advanced color image processing and analysis*: Springer, 2012, pp. 19-58.

[20] M. D. Fairchild, "A revision of CIECAM97s for practical applications," *Color Research & Application: Endorsed by Inter-Society Color Council, The Colour Group (Great Britain), Canadian Society for Color, Color Science Association of Japan, Dutch Society for the Study of Color, The Swedish Colour Centre Foundation, Colour Society of Australia, Centre Français de la Couleur,* vol. 26, no. 6, pp. 418-427, 2001.

[21] R. S. Berns, "Methods for characterizing CRT displays," *Displays,* vol. 16, no. 4, pp. 173-182, 1996.

[22] H. Yeganeh and Z. Wang, "Objective quality assessment of tone-mapped images," *IEEE Transactions on Image processing,* vol. 22, no. 2, pp. 657-667, 2012.

JOIN US AT THE NEXT EI!

electronic IMAGING

Imaging across applications . . . Where industry and academia meet!

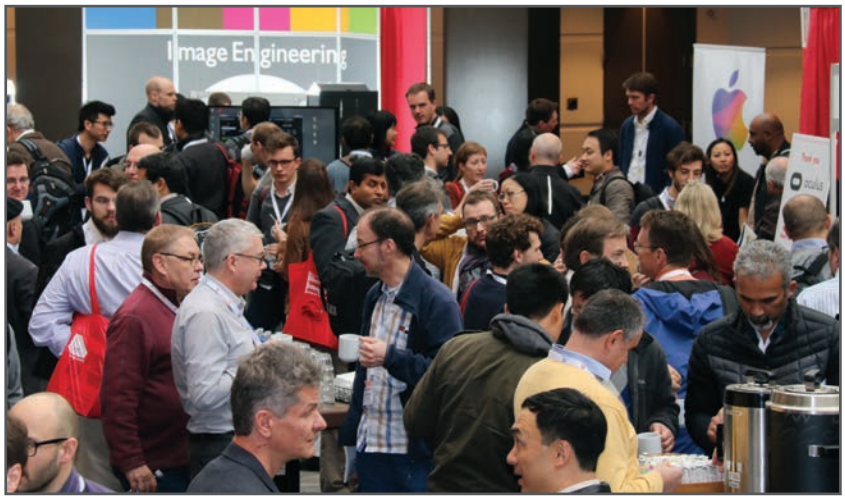

• SHORT COURSES • EXHIBITS • DEMONSTRATION SESSION • PLENARY TALKS •
• INTERACTIVE PAPER SESSION • SPECIAL EVENTS • TECHNICAL SESSIONS •

www.electronicimaging.org

ADVANCING IMAGING SCIENCE 75 1947 IS&T 2022 imaging.org